ELSEVIER

Journal of Nuclear Materials 258–263 (1998) 1803–1808

journal of nuclear materials

Production and recovery of defects in SiC after irradiation and deformation

J. Chen *, P. Jung, H. Klein

Institut für Festkörperforschung, Forschungszentrum Jülich, Association EURATOM-FZJ, D-52425 Jülich, Germany

Abstract

Changes of volume of thin silicon carbide specimens and a SiC/C composite and electrical resistivity of SiC were measured under helium implantation and during subsequent annealing. Comparison to proton irradiation shows that displacement defects are responsible for damage, while the implanted helium atoms play a minor role. Lattice dilatation and resistivity show rather different recovery behaviour, while annealing of dilatation after implantation and after deformation by polishing are amazingly similar. A tentative explanation of the recovery in terms of defect kinetics and reactions is given. © 1998 Elsevier Science B.V. All rights reserved.

1. Introduction

Silicon-carbide and SiC/C composite materials are under consideration for first wall and structural materials in future fusion reactors. Strong interatomic bonding, as indicated by the high melting point, causes at least one type of point defect to be immobile up to temperatures far above ambient. This leads to the retention of significant amounts of defects which causes lattice dilatation, and in the case of inhomogeneous damage large internal stresses. In the present work defect accumulation has been studied by measurements of electrical resistivity of thin ribbons and of their bending by irradiating to only about half of their thickness. The recovery behaviour of the defects was investigated by isochronal annealing experiments up to 1050°C. In addition the recovery behaviour of bending strains introduced by polishing was compared to those after inhomogeneous implantation, in an attempt to gain insight into the nature of the underlying defects.

2. Experimental

Polished sheets of 0.33–0.36 mm thickness of hot-pressed silicon carbide (SiC-HD, density: 3.2 g/cm^3, purity: $\geqslant$ 98.5%, electrical resistivity: 0.4–0.8 Ω m) were supplied by Elektroschmelzwerk Kempten. X-ray analysis showed a composition of 80% 6H–SiC, 18% 4H–SiC and 2% free C, while electron diffraction by transmission electron microscope (TEM) gave in addition 3C–SiC (β-SiC) and 15R–SiC in the percent range. The 6H–SiC had grain sizes from about 1 to 5 μm, while some of the 4H–SiC had a rod-type appearance with lengths up to 30 μm. The SiC/C particulate composite (SiC30, density: 2.65 g/cm^3, electrical resistivity: ≈200 μΩ m) was supplied by Schunk Kohlenstofftechnik GmbH in sheets of 0.32 mm. Chemical analysis gave a composition of 36.7 at% Si and 63.3 at% C and TEM showed mostly β-SiC. Both materials were cut into 40 mm long strips of $w = 2$ mm width. Specimen thicknesses were reduced by polishing to 200–300 μm for better resolution of the bending and resistivity measurements.

The specimens were soldered with Wood's metal to a copper heat sink, mounted in a vacuum chamber ($<10^{-3}$ Pa) behind a 28 μm aluminum window, and implanted at the Jülich compact cyclotron with 24.7 MeV α-particles. A rotating degrader wheel with 51 aluminum foils of appropriate thicknesses was used to obtain homogeneous helium implantation to maximum depths t_i of 96 μm in SiC-HD and 117 μm in SiC/C for both the bending and the resisitivity measurements. Specimen temperature during and after implantation was $\leqslant$ 80°C. For comparison to other irradiation environments the damage produced by helium implantation was trans-

* Corresponding author.

0022-3115/98/$19.00 © 1998 Elsevier Science B.V. All rights reserved.
PII: S0022-3115(98)00139-1

formed to displacement damage (dpa) by a factor 6×10^{-5} dpa/at. ppm He, cf. Ref. [1].

Bending strains due to irradiation of only about half of the specimen thickness were investigated by surface profilometry using a DEKTAK^{3}ST device with a 2.5 μm tip radius. The resolution of the measurements was mainly limited by surface roughness. Therefore specimens were polished before irradiation to a final roughness of $\leqslant 0.25$ μm with diamond paste. The implanted surface showed convex curvature (radius r) due to volume dilatation by irradiation defects. The calculation of linear strain ϵ ($= \triangle V/3V$) from r and thickness t_i of the implanted layer and total thickness t of the specimens was detailed in Ref. [1]:

$$\epsilon = \frac{t}{6rx(1-x)} \tag{1}$$

with $x = t_i/t$. The lateral compressive stress in the damaged layer σ_c is given by

$$\sigma_c = \frac{E't}{6rx}(1 - 3x + 6x^2). \tag{2}$$

$E' = E/(1-v)$ with E Young's modulus (445 GPa for SiC-HD and 140 for SiC/C) and v Poisson's ratio ($\approx$0.16).

For 4-point resisitivity measurement, 1 μm thick and 1 mm wide platinum contacts were sputtered onto the specimen strips after implantation to avoid impurity injection. Five sections of 5 mm length were thus obtained, the middle one coinciding with the 7 mm wide implanted region, while the others were used as references. The two adjacent sections also showed increases in resisitivity after implantation in the order of $\approx$10% of the middle region, due to beam spreading and misalignment. Resistance measurement was performed at room temperature in helium atmosphere with 30 and 50 μA measuring currents including current reversal to compensate for thermovoltages. Corrections for changes of geometry factor by irradiation induced expansion of typically 0.1% were not applied, considering the relative resistance changes in the order of 100%. The electrical resistivity of unimplanted SiC-HD showed an Arrhenius type temperature dependence from about 100°C to 600°C with an activation energy of about 0.3 eV and smaller slopes at temperatures outside this range. This activation energy falls into a range reported for p-type SiC [2]. The electrical resistivity of SiC/C is dominated by graphite. It is about one order of magnitude higher than that of typical graphites and also has a negative temperature coefficient.

For measurements of deformation effects two SiC-HD specimens of about 220 μm thickness were at first annealed at 1050°C to remove residual surface stresses from grinding by the supplier. Then they were polished on one side with 3 μm diamond paste, giving convex curvature which was investigated by thermal annealing. In all experiments isochronal annealing was performed in steps of 50°C or 100°C, with 1/2 h holding times.

3. Results

3.1. Production of irradiation damage

Fig. 1 shows strain of SiC-HD derived by Eq. (1) from the curvature produced by helium implanation into a surface layer. The data are compared to results from uniaxial elongation after transmittive proton irradiation at 265°C [1]. A cross section of 1.65×10^{-25} m^2 was used to convert proton doses to displacement damage [3,4]. The straining initially shows a linear dose dependence (power law exponent 1 ± 0.1) and eventually saturates at $\epsilon \approx 1\%$. The resolution of bending measurements on SiC/C was limited by the poor surface quality of this material even after polishing.

3.2. Annealing

Annealing of helium implanted SiC-HD and SiC/C specimens is shown in Fig. 2. The 200 atppm curve of SiC/C may be affected by microcracks due to the very high dose. Included are results for SiC after neutron irradiation from Refs. [5–7]. Recovery of reciprocal thermal conductivity after neutron irradiation [5,8] shows similar overall behaviour as the strains in Fig. 2. In contrast to the smooth recovery of dilatation, electrical resistivity shows a steep annealing step around 780°C (Fig. 3). Also after neutron irradiation annealing in a single step is observed, but already around 500°C [9]. The electrical resistivity of SiC/C shows only a minor increase after implantation if any, and consequently negligible recovery.

3.3. Polishing

As the thickness t_i of the damaged layer is not known, only the product $\sigma_c t_i \approx 780 \pm 30$ Pa m could be derived by Eq. (2) from the bending radius after polishing of SiC-HD with 3 μm diamond paste. For comparison implantation of 3.2 at. ppm helium in a 98 μm layer of 250 μm SiC-HD specimens produces an average $\sigma_c t_i \approx 770$ Pa m. The relative annealing of the bending strains are shown in Fig. 4.

4. Discussion

The agreement of the dilatation after helium implantation compared to transmittive proton irradiation indicates that straining is dominated by retained lattice defects while the implanted helium plays a negligible role. This is understandable as the implantation of one

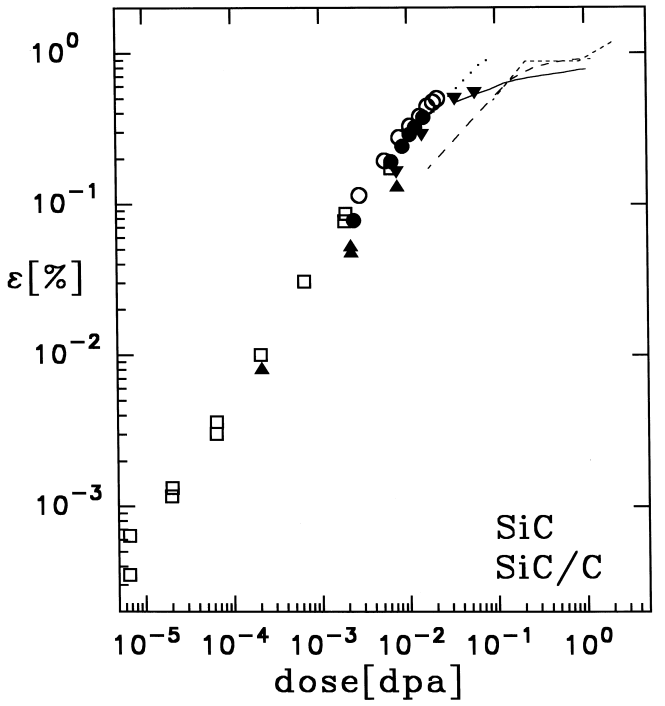

Fig. 1. Linear straining derived from bending measurements on SiC-HD (□) and SiC/C (▲,▼) during helium implantation at $\leqslant 80$°C [1] and from uniaxial length change of SiC-HD (○) and SiC/C (•) under proton irradiation at 265°C and 235°C as a function of displacement dose [3]. Included are results from lattice parameter and volume measurements on SiC under neutron irradiation at 250°C (-) [5], from 120°C to 180°C (· · ·) [12], from 120°C to 150°C (- -) [11], and at 200°C (– –) [10].

helium atom is accompanied by the production of about 60 Frenkel defects. Fig. 1 shows that also the dilatation derived from linear expansion [5] or from volume expansion [10–12] after neutrons irradiation is in good agreement with the present results. [1] This agreement also holds at higher temperatures, cf. Ref. [1].

More astonishing is the fact that for both particles the dilatation of SiC/C closely coincides with that of SiC-HD. This means that lattice expansion by defects in SiC/C is determined by the SiC component (60%), while the graphite is of minor importance. A possible reason could be that graphite in the dose range of Fig. 1 shows only negligible dimensional changes, mostly compaction, cf. Ref. [13], and therefore the specimen dimensions are dominated by the rigid SiC framework, to which the softer graphite accomodates itself.

From the derivatives of recovery of low-dose SiC-HD specimens, as given by the curves on the bottom of Fig. 2, annealing stages can be discriminated at $\leqslant 200$°C, ≈ 250°C, $\geqslant 530$°C and ≈ 800°C. The first stage seems to be independent of dose, while above 200°C recovery is strongly reduced with increasing dose. Therefore recovery below 200°C may be ascribed to close pairs, i.e. correlated recombination of interstitial–vacancy pairs without long-range migration. It may be speculated that the mobile species are carbon interstitials (I_C), as displacement of carbon atoms predominates due to their lower displacement energies, cf. a compilation in Ref. [14]. Furthermore computer simulations give migration energies for carbon interstitials of 1.3 eV [15], which would be an upper limit for the activation energy of the first-order close-pair recombination. The stage around 250°C may then be ascribed to free migrating I_Cs. Recovery in this temperatures regime has also been observed by positron annihilation spectroscopy (PAS) at low displacement doses [16,17]. At very low concentrations the I_C's may escape to grain boundaries, but at higher concentrations will be retained by clustering. A lower concentration limit c_I at which clustering becomes important can be estimated by comparing the formation rate of diinterstitials, i.e. the trapping rate of a mobile I_C at another I_C which is given by $4\pi r D_I c_I N_0$, and the average time needed to reach a grain boundary, $(s/8)^2/6D_I$. N_0, r and s are number density of the matrix atoms, reaction radius of I_C's and grain size, respectively. With $r \approx 10^{-10}$ m, $s \approx 10^{-6}$ m and $N_0 = 9.66 \times 10^{28}$ m^{-3},

[1] Neutron fluences were converted to dpa by a cross section of 7.3×10^{-26} m^2 [4].

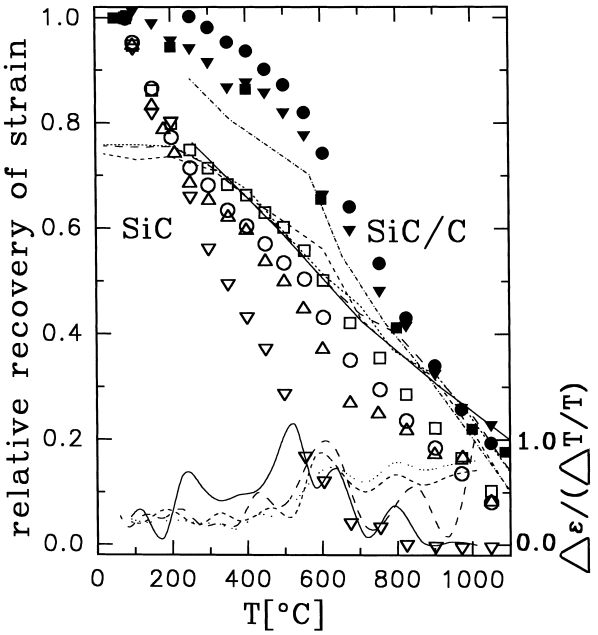

Fig. 2. Relative recovery of linear straining $\epsilon/\epsilon_0 = (l - l_0/l_i - l_0)$ derived from bending of SiC-HD after helium implantation to 1 (▽,-), 3.2 (△,– –), 10 (○,- -) and 30 atppm (≈0.0018 dpa, □,· · ·), and of SiC/C to 30 (▼), 100 (●) and 200 atppm (≈0.012 dpa, ■). The lines in the lower part of the figure are spline fits to the derivatives of the SiC-HD data, see right side ordinate. Included are results on annealing of dilatation after neutron irradiation of β-SiC at 250°C to 5.5×10^{24}/m^2 (≈0.04 dpa,——) [5], of SiC slightly above ambient to 4.3×10^{23}/m^2 (≈0.03 dpa, – • –) [6], and at 280°C to 8×10^{23}/m^2 (≈0.06 dpa), where short, medium and long dashes indicate reaction bonded, pressureless-sintered and hot-pressed SiC, respectively [7]. The data from Ref. [7] were normalized to the lengths after annealing around 1500°C. To match the present data, the data of Refs. [5,7] were multiplied by values of 0.76 and 0.75, corresponding to the irradiation temperatures of 250°C and 280°C, respectively.

clustering of interstitials occurs at $c_I \approx 10$ atppm, corresponding to an implanted He concentration of $\geqslant 0.2$ at. ppm ($c_I/c_{He} \leqslant 60$). This is in rough agreement with the value in Fig. 2 of about 1 at. ppm He.

The stages above 530°C and around 800°C may then be ascribed to the migration of vacancies. This assignment is mainly based on the observation of vacancy clustering by PAS [16] in this temperature regime after high-dose neutron irradiation where only rearrangement over short distances is needed. After electron irradiation at low displacement doses where migration over larger distances is needed for clustering, the PAS lifetime increases only above ≈900°C [17]. Furthermore computer calculations give migration energies for both Si and C vacancies around 2.7 eV [15] and differences between calculated formation energies [18] and measured self-diffusion energies of β-SiC [19,20] are also in this range. A defect annealing around 800°C observed by electron spin resonance (ESR) and photoluminescence (PL) was associated to the silicon vacancy [21,22], cf. also Ref. [23]. It is also above this temperature regime ($\geqslant$ 1000°C) that voids become visible after neutron irradiation [24]. Around 1250°C recovery may be complete when silicon interstitials become mobile. This is in agreement with the shrinking of vacancy clusters observed by PAS [16,17], and with calculated migration energies around 4.1 eV [15]. It is only above this temperature, when both types of interstitials are mobile, that dislocation loops form [25]. At temperatures above 1500°C, loops begin to coarsen [24] presumably by interstitial evaporation from the loops. Large remaining vacancy clusters (cavities) dissolve not below 1700°C [24] or at even higher temperatures [16], presumably by vacancy evaporation.

Fig. 2 shows that the relative recovery of dilatation in SiC after neutron irradiation (lines) to more than one order of magnitude higher displacement doses are in good agreement with the present high dose data, see also Ref. [12]. This means that cascade production has no marked effect on the contribution of defects to straining. Also an annealing experiment after neutron irradiation up to saturation of straining shows similar behaviour [25]. The smooth temperature dependence of strain recovery from 100°C to 800°C at high doses in Fig. 2 resembles that of strain saturation, which decreases almost linearly from room temperature to ≈900°C [26]. This also indicates that defect evolution is essentially determined by temperature and much less by defect concentration.

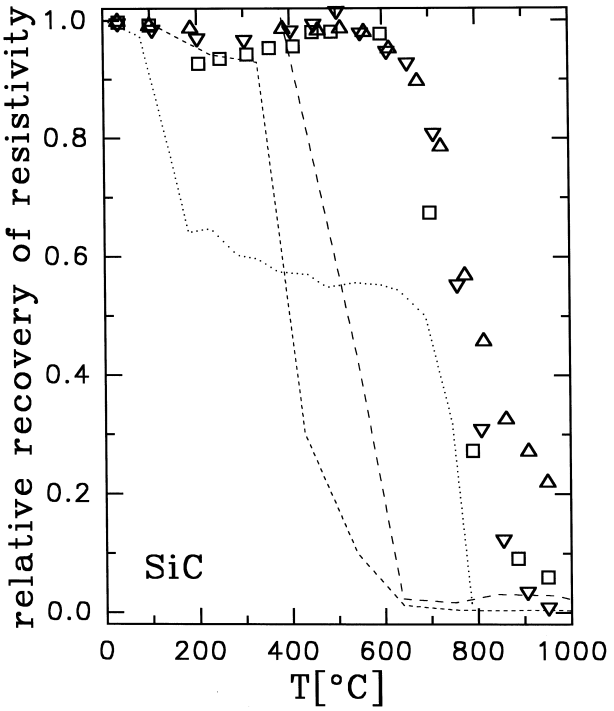

Fig. 3. Relative recovery of electrical resistivity $(\rho - \rho_0/\rho_i - \rho_0)$ of SiC-HD after implantation of 1 (▽), 10 (△) and 100 (□) atppm of helium. Included are recovery data of SiC after neutron irradiation to $2 \times 10^{23}/m^2$ (– –) and $2 \times 10^{24}/m^2$ (- -), respectively [9]. The dotted line gives the annealing of defect centers, measured by ESR [21].

SiC/C shows much less annealing below 200°C than SiC-HD at equal implantation dose. This is rather amazing when the almost identical defect production rates in Fig. 1 are considered. A tentative explanation could be the much higher fraction of β-SiC in SiC/C, i.e. less close pair production by larger interstitial-vacancy separation in the cubic structure.

The electrical resistivity in SiC-HD recovers in one major step around 780°C. Also after neutron irradiation resistivity recovers in one step, but at lower temperatures, which decrease with increasing dose [9] (Fig. 3). For other resisitivity measurements on neutron irradiated SiC see Refs. [27–29]. The lower annealing temperature for neutron irradiation conforms to the above mentioned behaviour of PAS lifetimes. If irradiation induced increase of resistivity is tentatively ascribed to the trapping of impurities or dopants at vacancies, the conductivity could recover by their dissociation when vacancies become mobile around 800°C. The annealing of ESR and PL signals which was ascribed to a silicon vacancy is included in Fig. 3 [21,22].

The annealing behaviour after polishing is similar to that after implantation to a similar $\sigma_c t_i$ product (≈780 Pa m in Fig. 2) as shown in Fig. 4. Only one study on surface damage induced by grinding of SiC is known to the authors [25]. In this investigation, TEM revealed only microcracks but no dislocations in the damaged region of 6H–SiC for abrasive particles smaller than 12 μm, while larger particles produced also dislocations on the {0 0 0 1} basal plane. Under careful treatment, the damaged region extended to a depth of only about one-tenth of the particle diameter. Only in a few investigations on other ceramics the residual stress induced by machining or grinding was measured as a function of depth in Al_2O_3 [30,31], MgO [32] and Si_3N_4 [33], while up to now no systematic investigation of the annealing of grinding damage has been performed. Only two qualitative results are available for Al_2O_3, indicating major recovery around 1200°C [31,34]. The above mentioned microstructural results for SiC and the present annealing behaviour indicate that careful polishing of SiC (and probably other ceramics) at room temperature produces point defects similar to irradiation but no extended defects.

5. Conclusions

1. Lattice dilatation by irradiation initially shows within experimental error a linear dose dependence and eventually saturates at $\epsilon \approx 1\%$.
2. Strains derived from inhomogeneous helium implantation, proton- and neutron irradiation agree when particle fluences are converted to displacement doses.

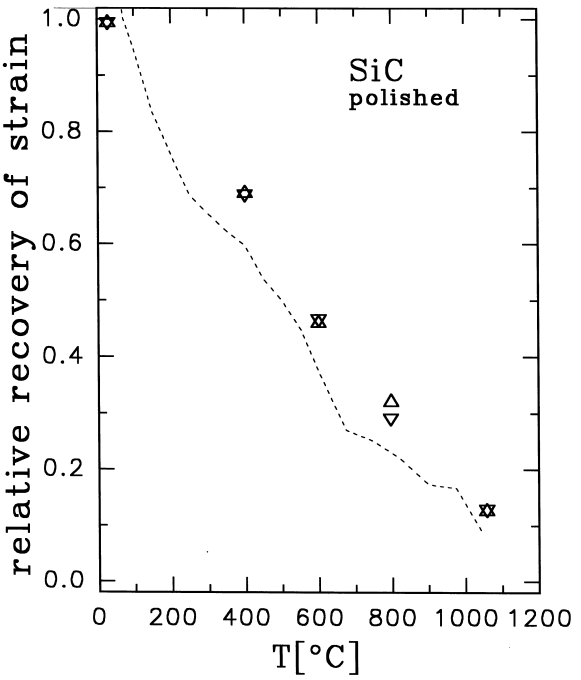

Fig. 4. Relative recovery of bending strain induced by one-side polishing of two ≈220 μm thick SiC-HD specimens (△,▽) with 3 μm diamond paste as a function of annealing temperature. The dashed line gives the annealing of the 3.2 atppm specimen in Fig. 2.

3. The straining of SiC/C is almost identical to that of pure SiC.
4. At low doses straining of SiC anneals in four stages at $\leqslant 200$°C, ≈250°C, $\geqslant 530$°C and ≈800°C.
5. Significant dose dependence is seen above the first stage.
6. The low temperature annealing stage ($\leqslant 200$°C) is almost completely missing in SiC/C.
7. The electrical resistivity of SiC recovers in one single step around 780°C with no discernible dose dependence.
8. SiC specimens deformed by polishing show annealing behaviour resembling that of specimens irradiated to a similar stress–depth product.

References

[1] P. Jung, Z. Zhu, J. Chen, J. Nucl. Mater 251 (1997) 276.
[2] P. Nagels, M. Denayer, in: Seventh International Conference on Phys. Semicond., Dunod, Paris, 1964 p. 225.
[3] Z. Zhu, Ph. D Thesis, Forschungszentrum Jülich, Jül-3109, 1995.
[4] Z. Zhu, P. Jung, J. Nucl. Mater. 212–215 (1994) 1081.
[5] R.P. Thorne, V.C. Howard, B. Hope, Proc. Br. Ceram. Soc. 7 (1967) 449.
[6] W. Primak, L.H. Fuchs, P.P. Day, Phys. Rev. 103 (1956) 1184.
[7] T. Suzuki, T. Yano, T. Maruyama, T. Iseki, T. Mori, J. Nucl. Mater. 165 (1989) 247.
[8] M. Rohde, J. Nucl. Mater. 182 (1991) 87.
[9] R.A. Matheny, J.C. Corelli, G.G. Trantina, J. Nucl. Mater. 83 (1979) 313.
[10] W. Dienst, J. Nucl. Mater. 211 (1994) 186.
[11] V.A. Nikolaenko, V.G. Gordeyev, V.N. Kuznetsov, Radiat. Effects 27 (1976) 163.
[12] N.F. Pravdyuk, V.A. Nikolaenko, V.I. Karpuchin, V.N. Kuznetsov, in: D.J. Littler (Ed.), Properties of Reactor Materials and the Effect of Radiation Damagem, Butterworths, London, 1962, p. 57.
[13] W. Delle, K. Koitzlik, H. Nickel, Graphitische Werkstoffe für den Einsatz in Kernreaktoren, Thiemig, vol. 1, 1979; vol. 2, 1983.
[14] S.J. Zinkle, C. Kinoshita, J. Nucl. Mater. 251 (1997) 200.
[15] H. Huang, N. Ghoniem, J. Wong, M. Baskes, Model. Simul. Mater. Sci. Eng. 3 (1995) 615.
[16] A.D. Mokrushin, A.I. Girka, A.V. Shishkin, Phys. Stat. Sol. (a) 128 (1991) 31.
[17] A.A. Rempel, H.-E. Schaefer, Appl. Phys. A 61 (1995) 51.
[18] C. Wang, J. Bernholc, R.F. Davis, Phys. Rev. B 38 (1988-I) 12752.
[19] M.H. Hon, R.F. Davis, J. Mater. Sci. 14 (1979) 2411.
[20] M.H. Hon, R.F. Davis, J. Mater. Sci. 15 (1980) 2073.
[21] H. Itoh, N. Hayakawa, I. Nashiyama, E. Sakuma, J. Appl. Phys. 66 (1989) 4529.
[22] H. Itoh, M. Yoshikawa, I. Nashiyama, J. Appl. Phys. 77 (1995) 837.
[23] L.A. de S. Balona, J.H.N. Loubser, J. Phys. C 3 (1970) 2344.
[24] R.J. Price, J. Nucl. Mater. 48 (1973) 47.
[25] H. Miyazaki, T. Suzuki, T. Yano, T. Iseki, Nucl. Sci. Technol. 29 (1992) 656.
[26] R. Blackstone, E.H. Voice, J. Nucl. Mater. 39 (1971) 319.
[27] V. Nagesh, J.W. Farmer, R.F. Davis, H.S. Kong, Appl. Phys. Lett. 50 (1987) 1138.
[28] P. Nagels, M. Denayer, in: Seventh International Conference on Phys. Semicond., Dunod, Paris, 1964, p. 225.
[29] H. Suzuki, T. Iseki, M. Ito, J. Nucl. Mater. 48 (1973) 247.
[30] B. Eigenmann, B. Scholtes, E. Macherauch, in: G. de With, R.A. Terptra, R. Metselaar (Eds.), Euro-Ceramics, vol. 3, Elsevier, Amsterdam, 1989, p. 3.554.
[31] F.F. Lange, M.R. James, D.J. Green, J. Am. Ceram. Soc. 66 (1983) C–16.
[32] E. Bernal, B.G. Koepke, J. Am. Ceram. Soc. 56 (1973) 634.
[33] D. Johnson-Walls, A.G. Evans, D.B. Marshall, M.R. James, J. Am. Ceram. Soc. 69 (1986) 44.
[34] B.J. Hockey, J. Am. Ceram. Soc. 54 (1971) 223.